Food and Agriculture Organization of the United Nations

Indian Ocean Tuna Commission
Commission des Thons de l'Ocean Indien

[IOTC-2026-WPB24-23]

CPUE STANDARDIZATION OF SWORDFISH (*XIPHIAS GLADIUS*) CAUGHT BY THE TAIWANESE LARGE-SCALE LONGLINE FISHERY IN THE INDIAN OCEAN USING SDMTMB

CHIH-YU LIN, WEN-QI XU, SHENG-PING WANG*[1]

Discussions: The paper is to inform meeting members of the sdmTMB standardized swordfish CPUE indices, as set out in Sections 2 and 3.

Feedback: The paper is to request review and comments on the model structure, fishing-strategy cluster effect, reference model, and resulting indices, as set out in Sections 2 and 3.

Conclusion: The paper is to seek confirmation of the 2005–2023 standardized CPUE series, as set out in Section 4.

Recommendation: The paper is to seek endorsement for considering the whole-ocean and regional indices as scientific inputs to swordfish stock assessment, as set out in Section 4.

Decisions: No formal approval is requested in this paper.

Department of Environmental Biology and Fisheries Science, National Taiwan Ocean University, Taiwan.
* Corresponding author: wsp@mail.ntou.edu.tw

Content:

Abstract

This study standardized catch-per-unit-effort (CPUE) for swordfish (Xiphias gladius) caught by the Taiwanese large-scale longline fishery in the Indian Ocean using a spatiotemporal model implemented in sdmTMB. Operational logbook records from 2005 to 2023 (602,219 fishing sets) were analyzed. Fishing strategy was represented by five clusters derived from hierarchical clustering of catch composition in the same 2005–2023 whole-Indian-Ocean operational dataset, thereby retaining fleet-wide operational heterogeneity without pre-stratifying the data by fixed fishing areas. Candidate sdmTMB models included delta-lognormal, delta-gamma, and Tweedie formulations and several mesh cutoffs. The 200-km delta-lognormal model was retained as the reference model and showed excellent numerical convergence, with 734 mesh vertices, a maximum final gradient of 2.82×10^{-9}, and all sdmTMB sanity checks passing. The standardized whole-Indian-Ocean index was relatively stable over 2005–2023 compared with nominal CPUE. In particular, the pronounced nominal increase in 2012 was substantially reduced after standardization. The standardized index reached its lowest value in 2017 (0.883) and its highest value in 2019 (1.185), and remained above the long-term mean in 2023 (1.107). Regional indices nevertheless showed substantial spatial heterogeneity, emphasizing the value of explicitly accounting for spatial and spatiotemporal processes when deriving abundance indices for stock assessment.

1. Introduction

Swordfish (*Xiphias gladius*) is an important component of the Indian Ocean tuna and billfish fisheries. During 2018–2022, longline fisheries accounted for approximately 53.6% of the total swordfish catch, and Taiwan contributed about 17% of the catch among flag States. The most recent stock assessment available in the source material indicated that the stock was not overfished and was not subject to overfishing at the whole-Indian-Ocean scale, while also highlighting potentially different regional trends, including concerns regarding the representativeness of rapidly increasing northern CPUE series and possible depletion in the southwestern Indian Ocean (IOTC, 2025).

Standardized CPUE is a key relative abundance input for stock assessment. For distant-water longline fisheries, however, nominal catch rates may be influenced by changes in fishing strategy, vessel effects, season, spatial allocation of effort, and the movement of fishing grounds through time. Spatiotemporal generalized linear mixed models provide a framework for estimating abundance indices while accounting for spatial dependence, uneven sampling, and spatiotemporal variation (Anderson et al., 2024).

The objective of this study was therefore to develop a standardized CPUE index for swordfish caught by the Taiwanese large-scale longline fishery throughout the Indian Ocean using sdmTMB. The analysis incorporated fishing-strategy clusters, vessel effects, seasonal effects, and spatial and spatiotemporal random fields. Whole-ocean and regional standardized indices were produced for use in IOTC stock assessment and related scientific discussions.

2. Materials and methods

2.1. Catch and effort data

Daily operational catch and effort logbook data for the Taiwanese large-scale longline fishery were provided by the Overseas Fisheries Development Council of Taiwan (OFDC). The broader 2026 data compilation covered the period from 1979 to 2025. Consistent with previous IOTC recommendations regarding the quality of early Taiwanese operational data, records before 2005 were excluded from CPUE standardization. The dataset used in the archived sdmTMB analysis comprised 602,219 fishing sets from 2005 to 2023. Swordfish catch was expressed as number of fish, while fishing effort was measured as the number of hooks and scaled to thousands of hooks in the model offset. Nominal CPUE was therefore expressed as fish per 1,000 hooks.

Swordfish catches were distributed throughout the Indian Ocean, but the principal catch and nominal CPUE hotspots occurred from the equatorial region northward into the northwestern Indian Ocean, including the Arabian Sea and waters off East Africa (Figs. 1–3). For descriptive fishery context, the updated project dataset for 2023–2025 indicated that the NW region accounted for approximately 60.7% of swordfish catch in numbers and 42.0% of fishing effort, and had the highest nominal CPUE at approximately 0.87 fish per 1,000 hooks. The four swordfish regions used for regional summaries followed Wang and Nishida (2011) (Fig. 1).

Historically, Taiwan classified longline vessels primarily by gross tonnage, designating vessels of 100 GT or greater as large-scale and those below 100 GT as small-scale. Following regulatory updates introduced beginning in 2021 to improve crew safety and onboard accommodations, several small-scale vessels exceeded 100 GT after structural modifications and were consequently reclassified as large-scale. However, many of these converted vessels retained operational characteristics typical of the small-scale longline fishery, including similar target species, fishing grounds, and operational practices. While the initial number of converted vessels was small and was expected to have only a limited influence on the large-scale fleet data, their numbers increased progressively thereafter, particularly in 2024 and 2025. Although the potential effect of this reclassification on CPUE was evaluated for other tuna species using data through 2023, a comparable evaluation for swordfish incorporating updated vessel information could not be completed within the available analytical timeframe. To avoid introducing additional uncertainty associated with shifts in fleet composition and catchability, the swordfish CPUE standardization presented here was restricted to data through 2023.

2.2. Fishing strategy and cluster analysis

Fishing strategy was characterized using the same 2005–2023 whole-Indian-Ocean operational dataset used for CPUE standardization. Catch composition for seven groups, albacore (ALB), bigeye tuna (BET), yellowfin tuna (YFT), swordfish (SWO), southern bluefin tuna (SBT), sharks (SKX), and other species (OTH), was clustered directly with the fastcluster framework using Ward's minimum-variance method and Euclidean distances (Müllner, 2013; Müllner, 2021).

The elbow criterion first fell below 10% at k = 5, and five clusters were retained (Fig. 4): an albacore-dominated group (Cluster 1), a bigeye-dominated group (Cluster 2), a yellowfin-dominated group (Cluster 3), a mixed multi-species group with appreciable swordfish, shark, and other-species contributions (Cluster 4), and an other-species-dominated group (Cluster 5; Table 1). Differences in swordfish catch and zero-catch proportion among clusters supported inclusion of cluster as a fixed effect in the CPUE model (Fig. 5).

2.3. Spatiotemporal CPUE standardization

CPUE was standardized with sdmTMB using a delta-lognormal generalized linear mixed model. The delta formulation represents the catch process by two linked components: a binomial submodel for the probability of encountering swordfish and a lognormal submodel for positive catches conditional on encounter. Both components included year and quarter as categorical fixed effects, fishing cluster as a fixed effect, and vessel identity as an independent and identically distributed random intercept. The logarithm of effort in thousands of hooks was included as an offset in the positive-catch component.

For fishing set i in year t at location s_i, the encounter component was represented as:

$$logit(p_{it}) = \beta_t^{(1)} + \gamma_{q(i)}^{(1)} + \delta_{c(i)}^{(1)} + b_{v(i)}^{(1)} + \omega^{(1)}(s_i) + \varepsilon^{(1)}(s_i, t)$$

and the positive-catch component was represented as:

$$log\{E(C_{it} \mid C_{it} > 0)\} = log(E_i) + \beta_t^{(2)} + \gamma_{q(i)}^{(2)} + \delta_{c(i)}^{(2)} + b_{v(i)}^{(2)} + \omega^{(2)}(s_i) + \varepsilon^{(2)}(s_i, t)$$

where p_{it} is encounter probability, C_{it} is swordfish catch in numbers, E_i is effort in thousands of hooks, β_t is the year effect, γq(i) is the quarter effect, δc(i) is the cluster effect, bv(i) is the vessel random effect, $\omega(s_i)$ is the persistent spatial random field, and $\varepsilon(s_i,t)$ is the spatiotemporal random field. Spatial random fields were represented through the stochastic partial differential equation (SPDE) approach with a Matérn covariance structure (Lindgren et al., 2011), and model estimation used Template Model Builder (TMB; Kristensen et al., 2016). Spatiotemporal random fields followed an AR(1) process, and geometric anisotropy was estimated.

The spatial domain was projected to a Lambert azimuthal equal-area coordinate system centered on the data domain. The reference model used a 200-km mesh cutoff, resulting in 734 mesh vertices (Fig. 6). Prediction was conducted on a 1° grid over the Indian Ocean. Bias-corrected response-scale predictions were integrated as area-weighted sums to obtain annual abundance indices. Whole-ocean and regional indices were standardized to a mean of one over the 2005–2023 period.

The annual standardized index can be expressed schematically as:

$$I_t = \sum_j A_j \hat{d}_{jt}, \quad I_t^* = I_t / \bar{I}$$

where A_j is the area represented by prediction-grid cell j, $\hat{d}_{jt}$ is the model-predicted density for cell j and year t, and I_t^* is the relative index after normalization by the mean index $\bar{I}$.

2.4. Candidate models and selection of the reference model

Candidate models included delta-lognormal (DL), delta-gamma (DG), and Tweedie (TW) formulations and DL models using 100-, 150-, and 200-km mesh cutoffs (Table 2). Convergence was evaluated using the maximum absolute gradient, Hessian and eigenvalue diagnostics, optimizer status, parameter-range checks, standard-error checks, and the sdmTMB sanity diagnostics.

The 200-km delta-lognormal model (cut_200_DL) was used as the reference model in this working paper, following the final model choice in the archived analysis. This choice should not be described as selection by minimum AIC: the finer 100-km DL model had a lower AIC, whereas the 200-km model provided a substantially smaller mesh and exceptionally strong numerical convergence. Importantly, the 150- and 200-km DL models produced nearly identical relative-index trajectories (r = 0.997), providing evidence that the temporal pattern was insensitive to these coarser mesh choices (Fig. 10).

3. Results and discussion

3.1. Fishery and fishing-strategy characteristics

Swordfish catches in the Taiwanese large-scale longline fishery declined substantially from the higher levels observed near the beginning of the study period. The broader Task 1 series summarized in the 2026 project report decreased from 6,898 t in 2005 to 2,081 t in 2023, with further decreases to 1,867 t in 2024 and 1,263 t in 2025. Spatially, catches and nominal CPUE were highest in the northwestern and low-latitude Indian Ocean, while lower but persistent fishing activity also occurred in the southern regions (Figs. 2–3).

The five clusters differed markedly in species composition and swordfish catch characteristics (Fig. 4; Table 1). Cluster 2 contributed a large share of swordfish catch in the earlier years, whereas Cluster 4 became more prominent later and generally showed relatively low zero-catch proportions (Fig. 5). In the selected sdmTMB model, Cluster 4 had the largest positive fixed-effect coefficient among the non-reference clusters for both encounter probability and positive catch rate, confirming an important fishing-strategy effect on swordfish catchability.

3.2. Model performance and spatial patterns

The selected cut_200_DL model converged satisfactorily with 602,219 observations and 65 estimated parameters. The maximum final gradient was 2.82×10^{-9}, the Hessian and eigenvalue checks passed, and all sdmTMB sanity diagnostics were successful. The model used 734 mesh vertices, substantially fewer than the 2,873 vertices in the 100-km models (Table 2). The delta-gamma and Tweedie 100-km candidates did not pass convergence diagnostics, whereas all three delta-lognormal mesh configurations converged.

Predicted density exhibited strong spatial structure throughout the study period (Fig. 7). Higher predicted density generally occurred in the northern, western-central, and equatorial Indian Ocean, consistent with the observed concentration of Taiwanese swordfish catch and CPUE. However, the distribution and intensity of high-density areas changed through time, indicating that a fixed spatial-stratum model could confound changes in fishing location with changes in relative abundance.

3.3. Standardized CPUE indices

The whole-Indian-Ocean standardized relative CPUE was comparatively stable over 2005–2023 (Fig. 8; Table 3). The most obvious effect of standardization occurred in 2012, when nominal relative CPUE showed a pronounced peak whereas the standardized index remained close to the long-term mean. This indicates that changes in encounter probability, fishing strategy, vessel composition, season, and spatial allocation contributed substantially to the nominal increase in that year.

The standardized index ranged from 0.883 in 2017 to 1.185 in 2019. It remained relatively high in 2020 (1.160), declined to 0.972 in 2022, and increased to 1.107 in 2023. Annual coefficients of variation were generally modest, approximately 7–9%, and the 2023 estimate had a 95% confidence interval of 0.961–1.276. These results do not suggest a persistent long-term decline in the whole-ocean standardized series over the modeled period.

Regional standardized indices nevertheless showed larger differences than the whole-ocean series (Fig. 9). The NW and NE regions fluctuated around the long-term mean with several peaks, the SW region was relatively high in the early part of the series before declining and later recovering, and the SE region increased in the most recent years. These contrasting trajectories reinforce the importance of retaining spatial structure in abundance-index estimation and are consistent with previous IOTC concerns about regional heterogeneity in swordfish abundance signals.

4. Conclusions

The sdmTMB analysis produced a stable whole-Indian-Ocean standardized CPUE index for swordfish from the Taiwanese large-scale longline fishery for 2005–2023 while explicitly accounting for fishing strategy, vessel effects, season, spatial dependence, and spatiotemporal variability. The selected 200-km delta-lognormal model showed excellent numerical convergence and a temporal trajectory highly consistent with the 150-km DL sensitivity model. The standardized series substantially reduced the large nominal CPUE anomaly in 2012 and showed no persistent monotonic decline over the modeled period, although regional indices differed considerably. The whole-ocean and regional indices presented here are suitable for consideration in IOTC stock-assessment analyses, with continued evaluation of mesh resolution, distributional assumptions, and incorporation of the most recent 2024–2025 operational data recommended in future updates.

Acknowledgements

This study was financially supported by the Fisheries Agency, Ministry of Agriculture, Taiwan (Grant No. 115AS-6.4.2-FA-02(1) to Sheng-Ping Wang).

References

Anderson, S.C., Ward, E.J., English, P.A., Barnett, L.A.K., and Thorson, J.T. 2024. sdmTMB: an R package for fast, flexible, and user-friendly generalized linear mixed effects models with spatial and spatiotemporal random fields. PLOS ONE. https://doi.org/10.1371/journal.pone.0305547.

He, X., Bigelow, K.A., and Boggs, C.H. 1997. Cluster analysis of longline sets and fishing strategies within the Hawaii-based fishery. Fisheries Research 31: 147–158.

IOTC. 2025. Report of the 23rd Session of the IOTC Working Party on Billfish. 15–18 September 2025, Sète, France. IOTC–2025–WPB23–R[E].

Kristensen, K., Nielsen, A., Berg, C.W., Skaug, H., and Bell, B.M. 2016. TMB: Automatic Differentiation and Laplace Approximation. Journal of Statistical Software 70(5): 1–21. https://doi.org/10.18637/jss.v070.i05.

Lindgren, F., Rue, H., and Lindström, J. 2011. An explicit link between Gaussian fields and Gaussian Markov random fields: the stochastic partial differential equation approach. Journal of the Royal Statistical Society Series B 73(4): 423–498. https://doi.org/10.1111/j.1467-9868.2011.00777.x.

Maunder, M.N., and Punt, A.E. 2004. Standardizing catch and effort data: a review of recent approaches. Fisheries Research 70: 141–159.

Müllner, D. 2013. fastcluster: Fast hierarchical, agglomerative clustering routines for R and Python. Journal of Statistical Software 53(9): 1–18.

Müllner, D. 2021. The fastcluster package: User's manual, Version 1.2.3.

Wang, S.P., and Nishida, T. 2011. CPUE standardization of swordfish (Xiphias gladius) caught by Taiwanese longline fishery in the Indian Ocean. IOTC–2011–WPB09–12.

Wang, S.P., Xu, W.Q., Lin, C.Y., and Kitakado, T. 2021. Analysis on fishing strategy for target species for Taiwanese large-scale longline fishery in the Indian Ocean. IOTC–2021–WPB19–11.

Figures

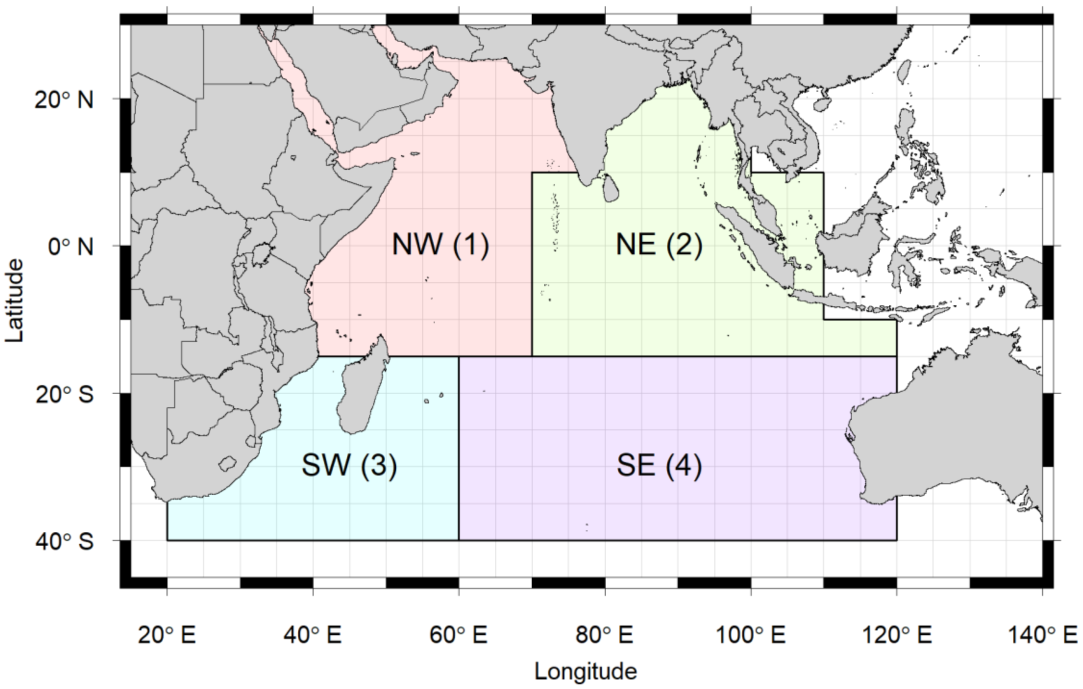

Fig. 1. Area stratification for swordfish in the Indian Ocean, following Wang and Nishida (2011).

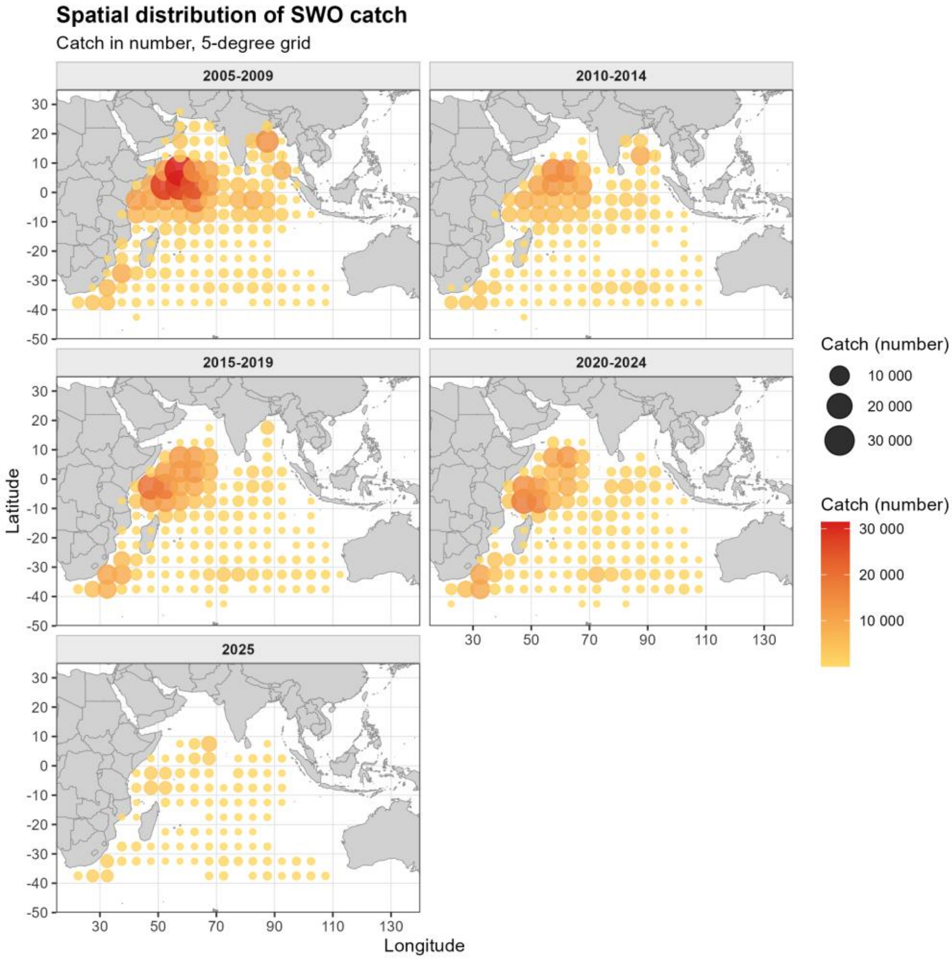

Fig. 2. Spatial distribution of swordfish catch by the Taiwanese large-scale longline fishery in the Indian Ocean.

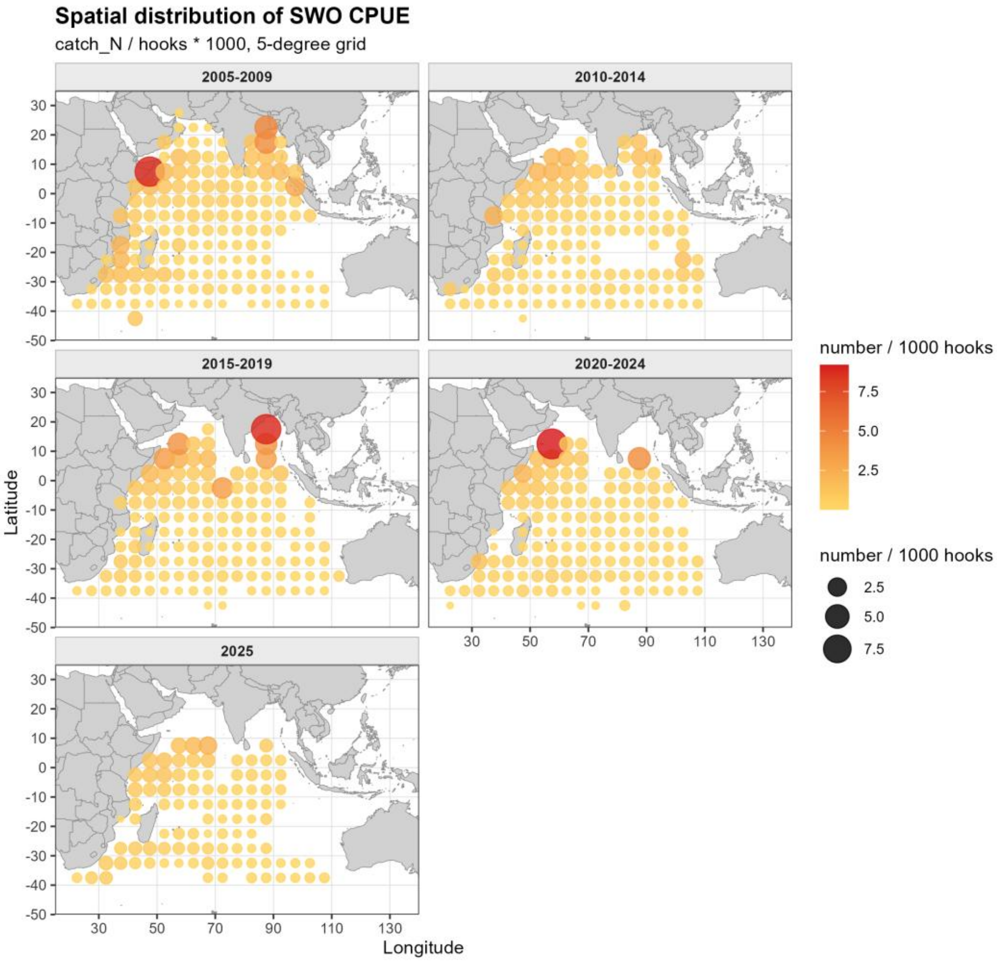

Fig. 3. Spatial distribution of nominal swordfish CPUE for the Taiwanese large-scale longline fishery in the Indian Ocean.

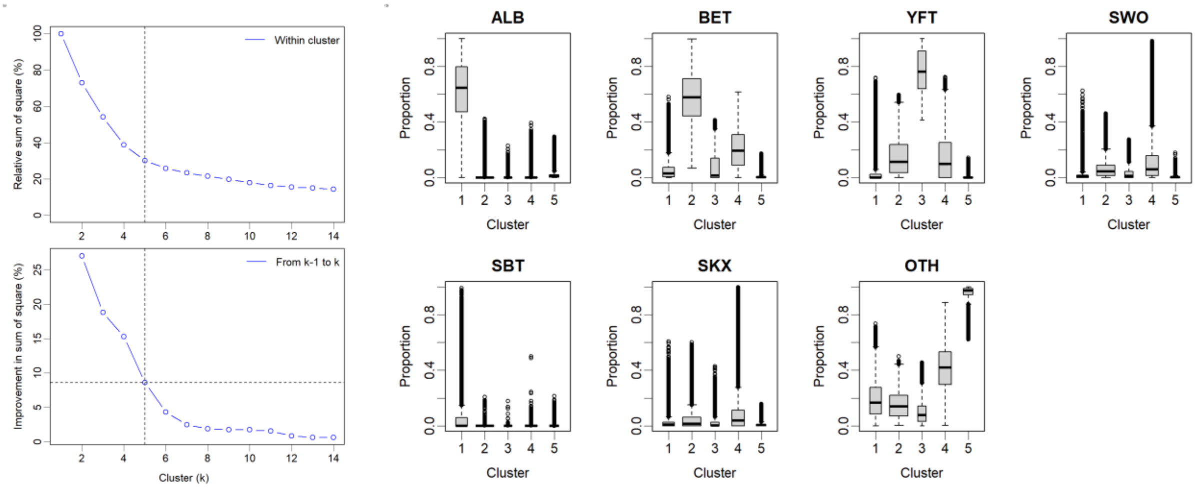

Fig. 4. Cluster analysis for the Taiwanese large-scale longline fishery in the whole Indian Ocean: (a) elbow analysis used to determine the number of clusters and (b) species-composition distributions by cluster.

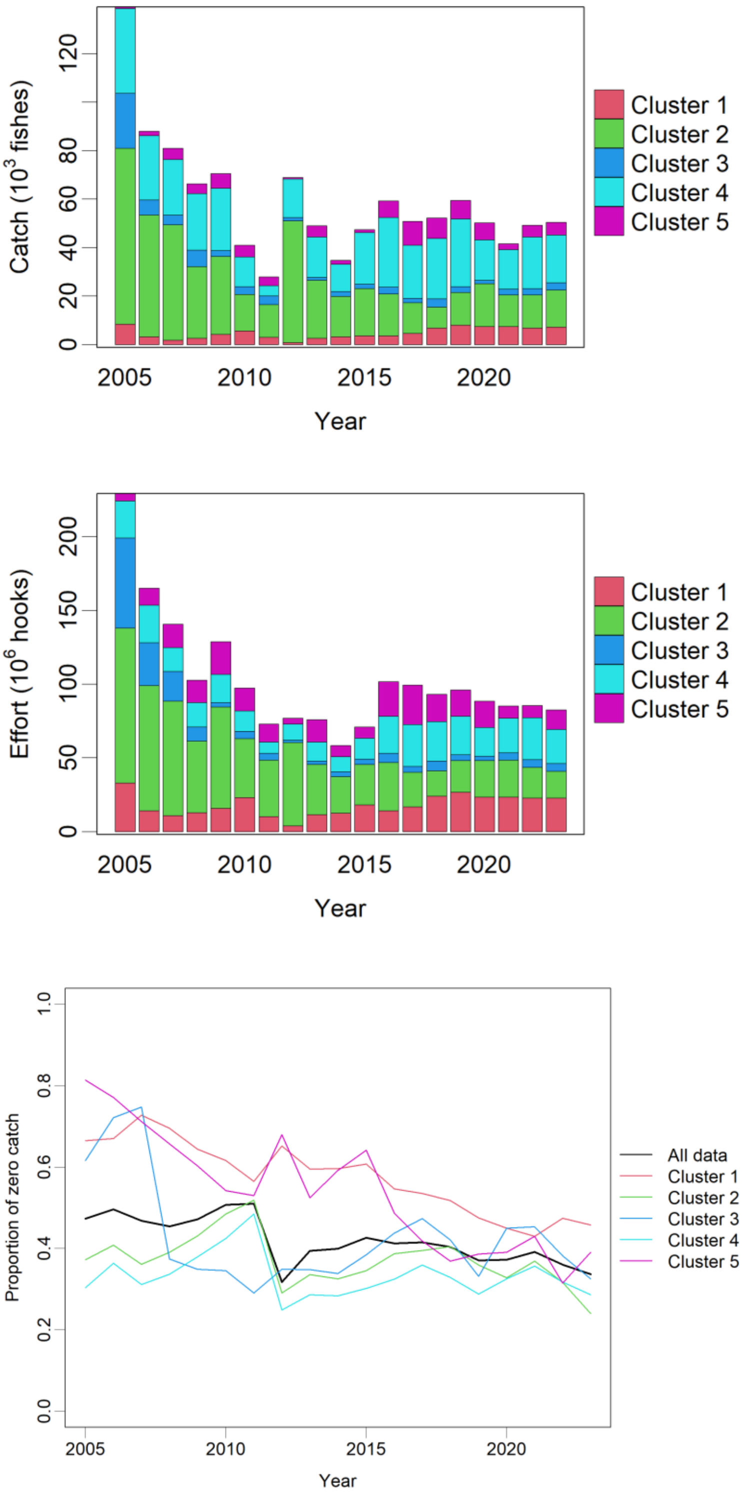

Fig. 5. Swordfish characteristics by fishing cluster: (a) annual swordfish catch and effort and (b) annual zero-catch proportion by cluster.

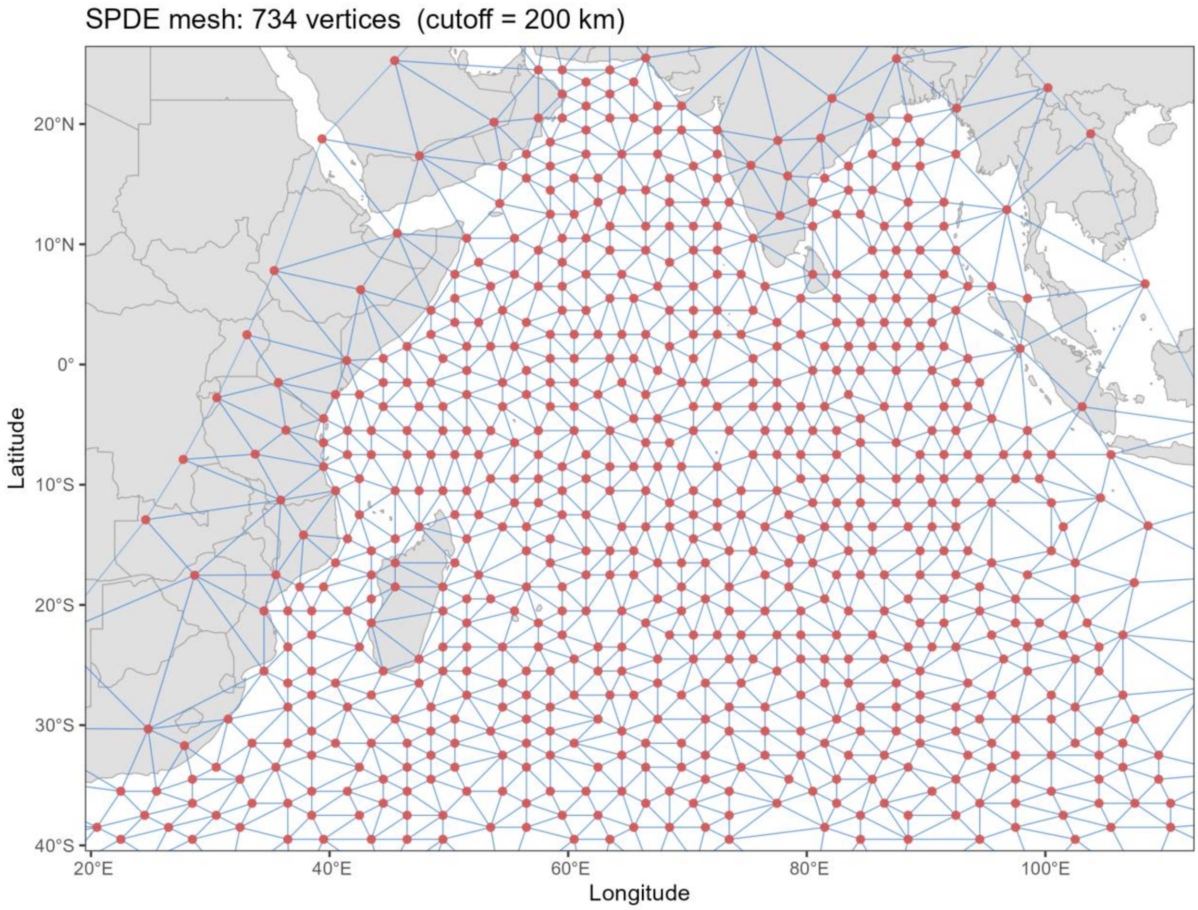

Fig. 6. SPDE mesh used for the selected 200-km delta-lognormal sdmTMB model (cut_200_DL). The mesh contained 734 vertices.

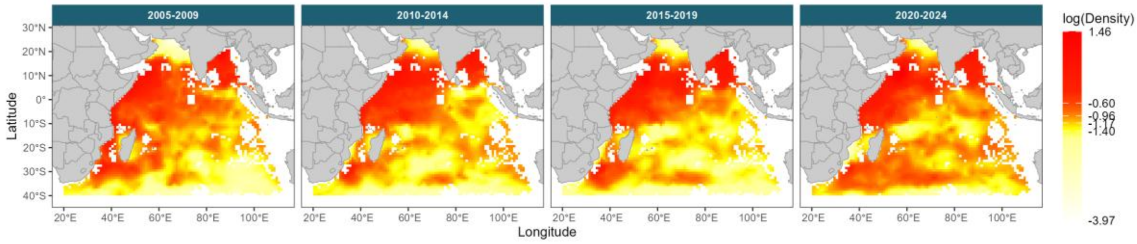

Fig. 7. Predicted swordfish density from the selected 200-km delta-lognormal sdmTMB model summarized in multi-year periods. The final plotted block is labelled 2020–2024 in the archived output, but the fitted dataset contains observations through 2023.

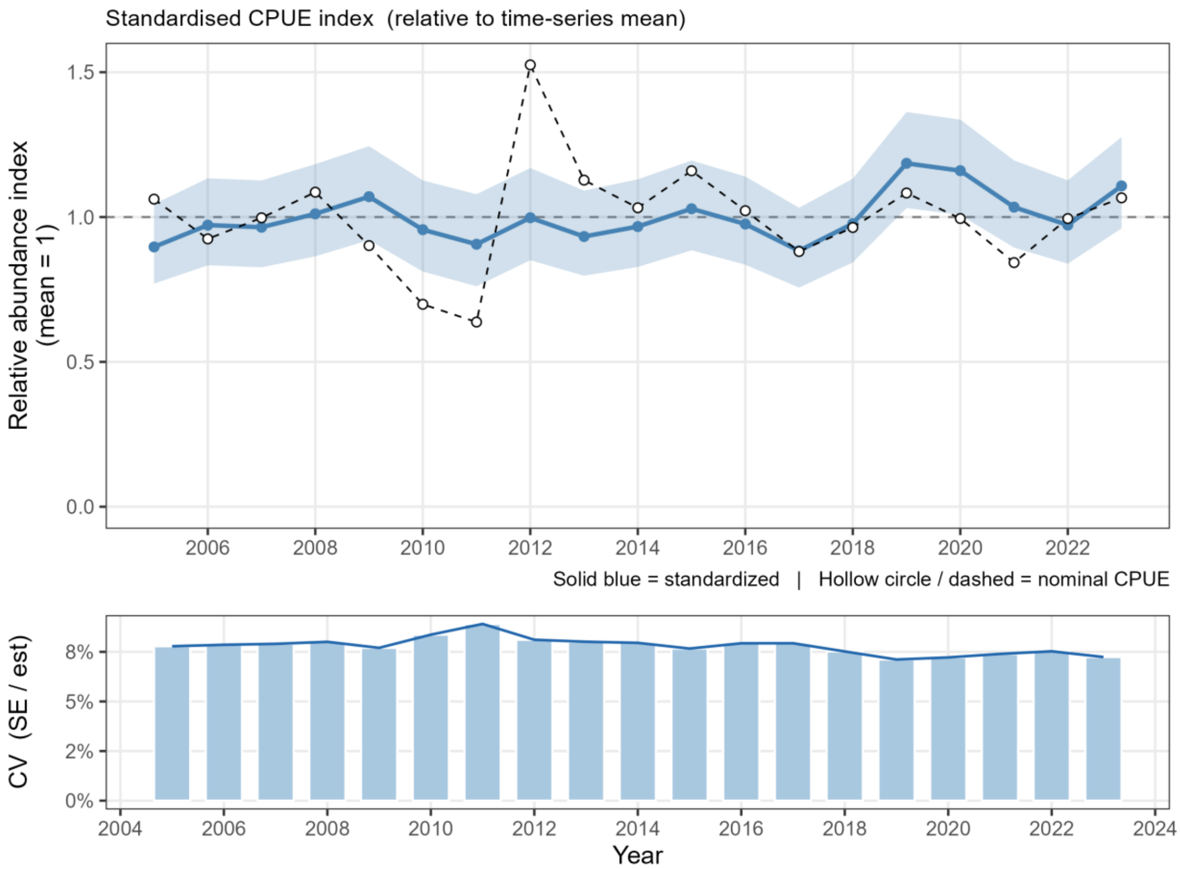

Fig. 8. Whole-Indian-Ocean relative standardized swordfish CPUE from the selected 200-km delta-lognormal sdmTMB model, compared with nominal relative CPUE, with annual coefficient of variation.

Fig. 9. Regional relative standardized swordfish CPUE indices and coefficients of variation for the NW, NE, SW, and SE Indian Ocean regions from the selected 200-km delta-lognormal sdmTMB model.

Fig. 10. Mesh-sensitivity comparison of whole-Indian-Ocean relative standardized CPUE among converged delta-lognormal models with 100-, 150-, and 200-km mesh cutoffs. The 150- and 200-km series were highly correlated (r = 0.997).

Tables

Table 1. Characterization of the five fishing-strategy clusters derived from the 2005–2023 whole-Indian-Ocean operational dataset and used as a fixed effect in the swordfish CPUE standardization model.

Cluster	Main characteristics	Preliminary operational interpretation
Cluster 1	Strongly dominated by albacore; albacore catch became more prominent toward the later years.	Albacore-targeting operations
Cluster 2	Dominated by bigeye tuna, with yellowfin tuna and other species also represented; contributed a large share of swordfish catch in the earlier years.	Bigeye-oriented tropical-tuna operations
Cluster 3	Strongly dominated by yellowfin tuna; total catch was concentrated mainly in the earlier years.	Yellowfin-targeting operations
Cluster 4	Mixed multi-species composition with substantial other-species catch and appreciable contributions from bigeye tuna, yellowfin tuna, swordfish, and sharks; increasingly important for swordfish in later years.	Mixed multi-species operations
Cluster 5	Overwhelmingly dominated by other species, with only minor contributions from the principal tuna and billfish groups.	Other-species-dominated operations

Table 2. Candidate sdmTMB model fit and convergence diagnostics for swordfish CPUE standardization. The selected reference model is cut_200_DL. AIC values are shown for diagnostic comparison and were not used as the sole selection criterion.

Model	Family	Cutoff (km)	Mesh vertices	Converged	Sanity	Max gradient	AIC
cut_100_DG	binomial / gamma	100	2873	No	Fail	1.10e-01	2,031,447
cut_100_DL	binomial / lognormal	100	2873	Yes	Pass	2.26e-05	1,988,957
cut_100_TW	tweedie	100	2873	No	Fail	2.07e-01	2,037,749
cut_150_DL	binomial / lognormal	150	1213	Yes	Pass	2.05e-05	1,991,007
cut_200_DL	binomial / lognormal	200	734	Yes	Pass	2.82e-09	1,992,575

Table 3. Whole-Indian-Ocean nominal and standardized relative swordfish CPUE indices from the selected cut_200_DL model, 2005–2023. Standardized indices are normalized to a time-series mean of 1.

Year	Nominal relative CPUE	Standardized index	95% CI lower	95% CI upper	CV
2005	1.062	0.897	0.770	1.044	0.078
2006	0.925	0.972	0.834	1.134	0.079
2007	0.997	0.965	0.827	1.126	0.079
2008	1.086	1.011	0.864	1.183	0.080
2009	0.901	1.070	0.921	1.244	0.077
2010	0.699	0.956	0.812	1.126	0.084
2011	0.638	0.906	0.761	1.079	0.089
2012	1.525	0.998	0.851	1.169	0.081
2013	1.127	0.933	0.798	1.091	0.080
2014	1.032	0.967	0.828	1.130	0.080
2015	1.160	1.029	0.885	1.195	0.077
2016	1.022	0.976	0.836	1.140	0.079
2017	0.881	0.883	0.756	1.032	0.079
2018	0.964	0.977	0.844	1.132	0.075
2019	1.083	1.185	1.031	1.363	0.071
2020	0.995	1.160	1.007	1.336	0.072
2021	0.843	1.034	0.895	1.195	0.074
2022	0.995	0.972	0.839	1.127	0.075
2023	1.066	1.107	0.961	1.276	0.072

Table 4. Regional standardized relative swordfish CPUE indices from the selected cut_200_DL model. Each regional series is normalized to its own time-series mean of 1.

Year	NW	NE	SW	SE
2005	0.830	0.919	1.157	0.817
2006	0.767	0.913	1.727	0.921
2007	0.880	1.131	1.018	0.903
2008	0.958	1.091	0.987	1.048
2009	1.140	1.093	0.864	1.046
2010	0.972	0.815	1.039	1.035
2011	0.911	0.745	0.923	1.086
2012	1.066	0.982	0.885	0.951
2013	0.982	0.889	0.853	0.940
2014	1.011	1.031	0.739	0.966
2015	1.144	1.160	0.726	0.841
2016	1.033	1.016	0.848	0.896
2017	0.861	0.922	0.949	0.834
2018	0.903	1.185	0.970	0.887
2019	1.197	1.287	1.105	1.095
2020	1.245	1.055	1.033	1.203
2021	1.041	0.936	0.972	1.191
2022	0.922	0.856	1.103	1.130
2023	1.138	0.975	1.101	1.212